Pages: 110 - 126 / Vol. 18 / Issue 2 / Summer- Fall 2025

**Journal of Aerospace Science and Technology**

Journal Homepage: https://jast.ias.ir

**Original Research Article**

# Effect of Viscous Heating on Heat Transfer and Entropy Generation inside a Partially Filled Porous Channel

**Mohammad Reza Salimi**

Aerospace Research Institute, Ministry of Science Research and Technology, Tehran, Iran

**TICLE INFO**

**Received:** 16 November 2024
**Revised:** 28 December 2024
**Accepted:** 08 January 2025
**Available online:** 23 September 2025

**KEYWORDS:**

Heat transfer
Porous media
Entropy generation
Second Law of Thermodynamics

**ABSTRACT**

The second laws of thermodynamics were investigated analytically for a two-dimensional, partially filled porous channel. The porous layer is attached to the channel walls in the first test case and inserted into the channel core in the second one. The flow is laminar, incompressible, and steady with constant wall temperature. Considering viscous dissipation effects, new analytical solutions for temperature, velocity, Bejan, and entropy generation number profiles were obtained. The results of the new analytical solutions were validated against the numerical results of the lattice Boltzmann method (LBM), which show very good agreement. Using these analytical solutions, a detailed analysis of the effects of the Brinkman number, Darcy number, and the porous layer thickness on entropy generation and Bejan numbers was carried out for the mentioned test cases. The results show that with the increase of Br and Da numbers for all investigated porous geometries, entropy generation, and Bejan numbers increase.

DOI:
https://doi.org/10.22034/jast.2025.487848.1212

## 1 INTRODUCTION

Since the porous media is used in many devices such as heat pipes, heat exchangers, cooling electronics, thermal insulation of homes, energy storage devices, oil resources, drying processes, and geothermal applications, etc., in recent decades, many scientists and researchers have researched forced heat transfer in porous media. Channels and pipes that are filled with porous media (fully or partially) are frequently used in the mentioned industries. Porous media in these devices is often used to increase the rate of heat transfer from the walls. For instance, Jiang et al. [1] conducted an experimental study on heat transfer in a fully filled porous channel. They also investigated this problem [2] numerically and showed that porous media have a significant impact on the increase in heat transfer. For instance, with the addition of the porous media, the local heat transfer coefficient for water and air is 15 and 30 times greater than for empty channels, respectively. The extra pressure drops (pumping power) caused by porous media are also very important engineering parameters in these devices. Thus, increasing the rate of heat transfer with a minimum rise in pressure loss is the most important design requirement in these devices. To

* Corresponding Author's Email: mohammadsalimi@ari.ac.ir

achieve this goal, the entropy analysis is a method that has been used by many researchers. Some of these researches are as follows:

For the first time, Bejan considered the second law of thermodynamics in different forced convection heat transfer problems and examined concepts like entropy generation number, distribution of irreversibility ratio, and entropy generation profiles on various issues [3-4]. Since then, a lot of research has been carried out on the profiles of entropy generation and irreversibility in different geometries, fluid streams, and boundary conditions. Because of nonlinear governing equations, most of them were analyzed numerically, and very few were solved analytically. Tasnima et al., in 2002 [5], according to the first and second laws of thermodynamics, analyzed heat transfer in a vertical channel fully filled with porous media under the influence of a magnetic field analytically. Allouache and Chikh in 2004 [6] analyzed entropy generation due to heat transfer and friction numerically in a double tube heat exchanger that is filled with porous media (fully and partially). Their goal was to find the optimal conditions that reduce the entropy generation. The effects of porous media thickness, permeability, and effective thermal conductivity are studied. Morosuk, in 2005 [7], examined the entropy generation due to fluid flow in a conduit partially filled with porous medium, analytically and numerically. The wall temperature of the conduit was constant. The flow was Laminar, and forced convection heat transfer was assumed. The effects of porous media thickness and permeability on the entropy generation rate were examined. However, the viscous dissipation was ignored. The results showed that for Da numbers greater than $10^{-4}$ analytical solution is very accurate. Moreover, the maximum entropy generation occurs at the porous plane interface, and its minimum is where the velocity becomes maximum. Mohamed et al. in 2011 [8] examined laminar forced convection heat transfer in a tube fully and partially filled with a porous media in three different cases. In this research, the effect of the viscous dissipation on the temperature profile was ignored. They studied the impact of the outer radius of the porous media and Da number on the velocity profile, local Nusselt, average Nusselt number, and pressure loss. They showed that, in the presence of the porous media, the average Nusselt number increases, and the hydrodynamic entrance length decreases. However, any increase in the radius of the porous layer over a critical value has a negative impact on the thermal performance and pumping power. Cimpean and Pop in 2011 [9] analyzed a mixed convection and entropy generation for a fluid flow through a porous medium between two inclined parallel plates. They developed analytic profiles for temperature and velocity and hence estimated the entropy generation. The optimum values of parameters such as Pecklet and Bejan numbers and the inclined angle were calculated by minimizing entropy generation. Hooman, in 2008 [10], studied fully developed flow in a channel filled with porous media numerically and analytically and showed that for small shape parameters (compared to unity), the velocity profile depends on the Forchheimer number. However, as the shape parameter increases, the central region containing a relatively uniform velocity distribution spreads further toward the walls, and the effects of form drag become less significant. Further, they indicated that, with an increase in either the Forchheimer number or shape parameters, the value of the Nusselt number increases.

Viscous dissipation has a significant impact on the temperature profile, heat transfer rate, and entropy generation number, especially in porous media problems. Nield [11] showed that in porous media problems, the effects of viscous dissipation depend on the ratio of the Brinkman number to the Darcy number. Since Darcy is almost a small number and it is placed in the denominator, this ratio is greater than unity, even for small Brinkman numbers. That is why the viscous dissipation is important in porous media. However, relatively few researchers have considered this parameter in the literature. Some of the research considering this parameter is listed below:

Mahmud and Fraser in 2005 [12] studied the fully developed forced convection and entropy generation in a fluid-saturated porous medium channel bounded by two parallel plates analytically and numerically. They mentioned the Darcy number as an important dimensionless parameter that affects the velocity and temperature profiles. After solving the governing differential equations with reasonable approximations, they obtained analytical relations for velocity, temperature, Nusselt number, entropy generation rate, and heat transfer irreversibility. The results indicated that, at low Darcy numbers, Nusselt and average Nusselt show a linear relationship with Darcy on a log-log graph. Additionally, results obtained by numerical calculations showed excellent agreement with analytical results.

Hooman and Ejlali, in 2007 [13], investigated the thermal development of forced convection in a circular tube filled with a saturated porous medium with uniform wall temperature. Effects of viscous dissipation were included. The temperature profile, Nusselt number, Bejan number, and the dimensionless entropy generation rate in the asymptotic region were obtained using the perturbation method. The perturbation method employed was previously developed by Hooman and Ranjbar-Kani in 2004 [14]. In 2007 [15], Abbassi analyzed the entropy generation in a uniformly heated microchannel heat sink (MCHS). They proposed analytical relations for local and average entropy generation rates in dimensionless form. The effect of parameters such as channel aspect ratio, group parameter, thermal conductivity ratio, and porosity on thermal and total entropy generation was investigated. Hooman et al. in 2008 [16] investigated entropy generation for thermally developing forced convection in a porous medium bounded by two isothermal parallel plates analytically based on the Darcy flow model. They took into account the viscous dissipation effects in their calculations. Chauhan and Kumar in 2009 [17] investigated fully developed forced convection in a circular channel filled with a highly porous medium saturated with a rarefied gas and uniform heat flux at the wall in the slip-flow regime. They formulated entropy generation due to heat transfer and fluid friction using the Darcy extended Brinkman-Forchheimer equation. The effects of slip and other parameters on the Nusselt number and entropy generation rate were examined. The results indicated that, for small slips at the wall, the velocity slip increases the Nusselt number, and the temperature slip decreases it. Additionally, the total entropy generation number attains high values in the region close to the duct walls. In 2011 [18], they investigated the characteristics of the first and the second law of thermodynamics in a compressible fluid flow inside a composite channel partially filled with a porous medium. They obtained velocity distribution, temperature distribution, rate of heat transfer, entropy generation number, and Bejan number for both porous and clear fluid regions analytically. The focus of this study was on the viscous dissipation effects on heat transfer. In 2013 [19], they investigated a non-Newtonian third-grade fluid flow in an annulus partially filled by a porous medium of very small permeability. Velocity and temperature fields were solved analytically by the perturbation series method. They assumed Reynolds's model to consider the variation of fluid viscosity with temperature. All calculations in the three papers were performed by considering viscous dissipation completely (including Darcy and Brinkman terms) [17-19]. Makinde and Eegunjobi in 2013 [20] numerically studied the combined effects of convective heating and suction/injection on the entropy generation rate in a steady flow of an incompressible viscous fluid through a channel with permeable walls. The effects of the influential parameters like Reynolds, Eckert, Prandtl, and lower and upper walls Biot numbers on the fluid velocity, temperature, entropy generation rate, and Bejan number were analysed. They showed that the entropy generation rate increases with increasing values of the lower and upper walls Biot numbers. Additionally, an increase in Re decreases the Bejan number at the lower wall region and increases it at the upper wall region.

Kamish in 2009 [21], analytically examined the flow of an incompressible fluid confined in a planar geometry that is filled with a homogenous and isotropic porous medium. The effects of viscous dissipation were included in their analysis. They determined the unsteady state and steady state velocities, the temperature, and the entropy generation rate as a function of the pressure drop, Darcy number, and Brinkman number. They found that these parameters affect the temperature distribution in a similar way. Moreover, they showed that the deviation from the linearity of the temperature profile increases with increasing Darcy and Brinkman numbers. Hooman et al. in 2008 [22] investigated the entropy generation due to forced convection in a plane channel filled by a saturated porous medium numerically. Viscous dissipation was entirely considered in their model. They found that regardless of the boundary condition, increasing the porous media shape factor and the Brinkman number and decreasing the dimensionless heat flux or temperature difference increases the dimensionless degree of irreversibility of the problem.

Salimi et al. investigated the flow and heat transfer from a porous cylinder and a rigid cylinder covered with a layer of porous medium by a hybrid lattice Boltzmann-Navier-Stokes method [23-26]. In another study, they investigated the interaction between a porous layer and an impinging jet from the perspective of the second law of thermodynamics [27]. In addition, they have conducted research on rarefied gas flow inside porous media [28-29].

Zahor et al. in 2023 [30] and Mebarek-Oudina et al. in 2024 [31] researched the entropy production of nanofluids in a porous medium under the influence of a magnetic field. Their research was conducted with the aim of investigating the performance of thermal systems under the influence of a magnetic field.

To the best of the author's knowledge, there is no analytical solution in the literature for flow and heat transfer in a channel partially filled by porous media, including the Brinkman term in the momentum equation and the viscous dissipation term in the energy equation. Thus, in the present research, an analytical solution is developed to analyze temperature and velocity fields in a channel that is partially and fully filled with porous media. As mentioned before, the Brinkman term in the momentum equation and the viscous dissipation term in the energy equation are considered. Based on the obtained profiles for temperature and velocity, the entropy generation number and Bejan number are calculated analytically. Then, the effects of parameters such as Darcy number, Brinkman number, and thickness of the porous media on Bejan and entropy generation numbers are analyzed in detail.

## 2 GOVERNING EQUATIONS

In this section, the momentum and energy equations are presented in non-dimensional form for flow inside and outside of the porous medium. Additionally, the entropy generation equation in heat transfer problems, including porous media, is described. Definitions for entropy generation and Bejan numbers are also presented here.

**Momentum and Energy Equations:** The two-dimensional momentum and energy equations for thermally fully developed flow inside a channel partially filled with porous material are as follows:

$$\frac{\partial^2 u}{\partial y^2} = -\frac{1}{Da}u - Re\left(\frac{\partial p}{\partial x}\right), \quad \text{in porous} \qquad (1)$$

$$\frac{\partial^2 u}{\partial y^2} = -Re\left(\frac{\partial p}{\partial x}\right), \quad \text{in Fluid} \qquad (2)$$

$$\frac{\partial^2 \theta}{\partial y^2} = -Br\left[\frac{u^2}{Da} + \left(\frac{\partial u}{\partial y}\right)^2\right], \quad \text{in porous} \qquad (3)$$

$$\frac{\partial^2 \theta}{\partial y^2} = -Br\frac{k_{eff}}{k_f}\left(\frac{\partial u}{\partial y}\right)^2, \quad \text{in Fluid} \qquad (4)$$

where $k_{eff}$ and $k_f$ are the effective conduction coefficient in porous media and the conduction coefficient of fluid, respectively. In the above equations, the independent and dependent variables are non-dimensioned as:

$$\theta = \frac{T - T_c}{T_h - T_c} = \frac{T - T_c}{\Delta T}, \quad U_i = \frac{u_i}{U_c}, \quad X_i = \frac{x_i}{L}, \qquad (5)$$

where $T_h$, $T_c$, $L$ and $U_c$ are the maximum temperature, minimum temperature, characteristic length, and characteristic velocity scales, respectively. Additionally, the flow Reynolds number $\mathrm{Re}$, Darcy number $Da$, and Brinkman number $Br$ are defined as follows:

$$\mathrm{Re} = \frac{\rho U_c L}{\mu}, \quad Da = \frac{K}{L^2}, \quad Br = \frac{\mu U_c^2}{k_{eff}\Delta T}, \qquad (6)$$

where K is permeability.

**Entropy Generation Equations in Fluid Region:** Based on Bejan descriptions, fluid viscosity, and its related losses, as well as heat transfer, are two main sources of irreversibility in heat transfer problems. On this basis, the following formula for the entropy generation is presented [32].

$$S''' = \frac{k}{T_0^2}\left(\frac{\partial T}{\partial x_i}\right)^2 + \frac{\mu}{T_0}\left[2\left(\frac{\partial u_i}{\partial x_i}\right)^2 + \left(\frac{\partial u_i}{\partial x_j} + \frac{\partial u_j}{\partial x_i}\right)^2\right] \qquad (7)$$

where $\mu$ is fluid viscosity, and $k$ is the heat conduction coefficient. Bejan divided the above equation by a characteristic rate of entropy generation, defining the non-dimensional entropy generation rate. Therefore, he introduced the number of entropy generation as a measure of performance in engineering systems. The characteristic rate of entropy generation is as follows:

$$S_C = \left[\frac{q^2}{kT_0^2}\right] = \left[\frac{k(\Delta T)^2}{L^2 T_0^2}\right] \qquad (8)$$

where $q$ is the rate of heat transfer, $L$ is the characteristic length, $T_0$ is the reference temperature, and $\Delta T$ is the characteristic temperature difference. The first part in Eq. (8) is used when heat flux is defined, and the second part is used when temperature difference is defined. Now, dividing Eq. (7) by Eq. (8), the entropy generation number is obtained as:

$$N_t=\left(\frac{\partial\theta}{\partial X_i}\right)^2+\frac{Br}{\Omega}\left[2\left(\frac{\partial U_i}{\partial X_i}\right)^2+\left(\frac{\partial U_i}{\partial X_j}+\frac{\partial U_j}{\partial X_i}\right)^2\right], \quad (9)$$

where $\Omega$ is the group parameter, and defined as:

$$\Omega=\frac{\Delta T}{T_0} \quad (10)$$

As mentioned previously, the first term in Eq. (9) is the irreversibility due to the thermal conductivity, and the second term is the irreversibility due to friction. In many engineering problems, identifying the contribution of each of these two terms is important. Irreversibility distribution ratio ($\varphi$) is a non-dimensional number that defines the contribution of each of these two terms. This number is the ratio of viscous irreversibility to heat transfer one. Another important non-dimensional number is the Bejan number. This number is the ratio of entropy generation due to heat transfer to the total entropy generation. The Bejan number is identified with Be and is related to the irreversibility distribution ratio "$\varphi$" as below:

$$Be=\frac{1}{1+\phi} \quad (11)$$

Therefore, "Be" changes from zero to one. When this number is close to zero, indicating the dominance effects of viscosity and friction losses, and whenever it is close to one, the contribution of heat transfer in entropy generation increases.

**Entropy Generation Equation in Porous Media:** The entropy generation term in porous media is calculated as follows [11]:

$$S'''=\frac{k_{eff}}{T_0^2}\left(\frac{\partial T}{\partial x_i}\right)^2+\frac{\mu}{T_0}\left[\frac{1}{K}u_i^2+2\left(\frac{\partial u_i}{\partial x_i}\right)^2+\left(\frac{\partial u_i}{\partial x_j}+\frac{\partial u_j}{\partial x_i}\right)^2\right]. \quad (12)$$

where $u_i$ is Darcy's velocity. The last two terms in Eq. (12) are suggested by Al-Hadhrami [33] to modify the behavior of the model in large Darcy numbers and at a porous-plane interface. With the addition of these terms, the presented model reduces to Eq. (7) in free flow since the permeability coefficient goes to infinity in free flow. Note that Eq. (12) is derived with the assumption of local thermodynamic equilibrium in porous media, regardless of the heat dispersion effects. Now, by dividing Eq. (12) by Eq. (8) and substituting the non-dimensional relations Eqs. (5-6), the entropy generation number is obtained as follows:

$$N_t=\left(\frac{\partial\theta}{\partial X_i}\right)^2+\frac{Br}{\Omega}\left[\frac{1}{Da}U_iU_i+2\left(\frac{\partial U_i}{\partial X_i}\right)^2+\left(\frac{\partial U_i}{\partial X_j}+\frac{\partial U_j}{\partial X_i}\right)^2\right] \quad (13)$$

As shown in Eq. (13), the first term in the bracket is divided by Darcy's number. This term represents the viscous dissipation in porous media. Since the Darcy number is usually small in porous materials, viscous dissipation is more important in porous media compared to free flow [34]. Note, since in the present research, the Reynolds number inside porous media is assumed very low, the contribution of the Forchimer term in viscous dissipation is neglected.

## 3 PROBLEM DESCRIPTION AND VALIDATION

In this section, the problem description and boundary conditions for three-channel geometries are presented. In the first case, the channel walls are coated with porous media. In the second case, the porous insert is located in the middle of the channel, and in the third case, the channel is filled completely with porous media. To validate the proposed analytical solutions, the profiles of temperature, velocity, Bejan, and entropy generation numbers are compared with the numerical results of the lattice Boltzmann method. The D2Q9 model with a multiple relaxation times collision operator has been used to simulate the flow field, while the temperature field is simulated using the second-order upwind finite volume method.

**Channel with porous coating on the walls:** The schematic of problem geometry and boundary conditions are shown in Fig. 1. To solve the momentum equations in porous media and flow field, two equations for near walls porous layers (Eq. 1) and one equation for the central plane region (Eq. 2) are solved. By solving these equations, six constants appeared, which can be found from boundary conditions such as no-slip wall boundaries and velocity and shear stress continuity at the porous-plane interfaces. Therefore, the unknown constants are determined, and the resulting analytical solutions for plane and porous regions are as follows:

$$u_f=-\mathrm{Re}\frac{\partial p}{\partial x}\left(\begin{array}{l}\frac{y^2}{2}+Da\cdot\operatorname{sech}\left[\frac{s-1}{\sqrt{Da}}\right]+\\ s\cdot\sqrt{Da}\tanh\left[\frac{s-1}{\sqrt{Da}}\right]-\left[Da+\frac{s^2}{2}\right]\end{array}\right) \quad (14)$$

$$u_p = -B_1 \sinh\left(\frac{|y|}{\sqrt{Da}}\right) - B_2 \cosh\left(\frac{y}{\sqrt{Da}}\right) + Da\,\mathrm{Re}\frac{\partial p}{\partial x} \tag{15}$$

where $u_p$ Darcy velocities are in porous and plain regions, respectively. The constants of $B_1$ and $B_2$ are determined as follows:

$$B_1 = \sqrt{Da}\,Re\frac{\partial p}{\partial x}\left(\sqrt{Da}\,\frac{\sinh\left[\frac{s}{\sqrt{Da}}\right]}{\cosh\left[\frac{s-1}{\sqrt{Da}}\right]} - s\cdot\frac{\cosh\left[\frac{1}{\sqrt{Da}}\right]}{\cosh\left[\frac{s-1}{\sqrt{Da}}\right]}\right) \tag{16}$$

$$B_2 = \sqrt{Da}\,\mathrm{Re}\frac{\partial p}{\partial x}\left(\sqrt{Da}\,\frac{\cosh\left[\frac{s}{\sqrt{Da}}\right]}{\cosh\left[\frac{s-1}{\sqrt{Da}}\right]} - s\cdot\frac{\sinh\left[\frac{1}{\sqrt{Da}}\right]}{\cosh\left[\frac{s-1}{\sqrt{Da}}\right]}\right) \tag{17}$$

Now, the $\partial u/\partial y$ terms (in porous and plain regions) and (in the porous region) can be calculated from Eqs. (14-17). By substituting these terms into Eqs. (3-4) and integrating, the analytical solution for temperature can be derived as follows:

$$\theta_L = -Br\left\{\begin{array}{l}\frac{B_1^2+B_2^2}{4}\cosh\left(\frac{2y}{\sqrt{Da}}\right)- \\ 2B_2\,\mathrm{Re}\,Da\frac{\partial p}{\partial x}\cosh\left(\frac{y}{\sqrt{Da}}\right)+\frac{1}{2}\mathrm{Re}^2\,Da\left(\frac{\partial p}{\partial x}\right)^2 y^2\end{array}\right\} -Br\left\{\begin{array}{l}\frac{B_1\cdot B_2}{2}\left[\sinh\left(\frac{2y}{\sqrt{Da}}\right)-\frac{2y}{\sqrt{Da}}\right]- \\ 2B_1\,\mathrm{Re}\,Da\frac{\partial p}{\partial x}\sinh\left(\frac{y}{\sqrt{Da}}\right)\end{array}\right\}+F_1y+F_2 \tag{18}$$

$$\theta_M = -\frac{1}{12}\left(\frac{k_{eff}}{k_f}\right)Br\,\mathrm{Re}^2\left(\frac{\partial p}{\partial x}\right)^2 y^4 + H_1y + H_2 \tag{19}$$

$$\theta_H = -Br\left\{\begin{array}{l}\frac{B_1^2+B_2^2}{4}\cosh\left(\frac{2y}{\sqrt{Da}}\right)- \\ 2B_2\,\mathrm{Re}\,Da\frac{\partial p}{\partial x}\cosh\left(\frac{y}{\sqrt{Da}}\right)+\frac{1}{2}\mathrm{Re}^2\,Da\left(\frac{\partial p}{\partial x}\right)^2 y^2\end{array}\right\} +Br\left\{\begin{array}{l}\frac{B_1\cdot B_2}{2}\left[\sinh\left(\frac{2y}{\sqrt{Da}}\right)-\frac{2y}{\sqrt{Da}}\right]- \\ 2B_1\,\mathrm{Re}\,Da\frac{\partial p}{\partial x}\sinh\left(\frac{y}{\sqrt{Da}}\right)\end{array}\right\}+E_1y+E_2 \tag{20}$$

where $\theta_H$ $\theta_L$ are the temperature equations for upper and lower channel walls, respectively, and $\theta_M$ is the temperature in the channel central region (plain region). The six constants of $F_1$, $F_2$, $E_1$, $E_2$, $H_1$ and $H_2$ can be determined by satisfying constant temperature boundary conditions on channel walls, as well as temperature and heat flux continuity at porous-plain interfaces. Thus, the constants are calculated as follows:

$$H_1 = \frac{\theta}{2\left(\frac{k_f}{k_{eff}}\right)(1-s)+2s} \tag{21}$$

$$F_1 = \frac{k_f}{k_{eff}}H_1 + \frac{1}{3}Br\,\mathrm{Re}^2\left(\frac{\partial p}{\partial x}\right)^2 s^3 + M(S) \tag{22}$$

$$E_1 = \frac{k_f}{k_{eff}}H_1 - \frac{1}{3}Br\,\mathrm{Re}^2\left(\frac{\partial p}{\partial x}\right)^2 s^3 - M(S) \tag{23}$$

$$F_2 = F_1 - \omega(1) \tag{24}$$

$$E_2 = \theta - \omega(1) - E_1 \tag{25}$$

$$H_2 = F_2 + s(H_1 - F_1) + \omega(s) + \frac{1}{12}\left(\frac{k_{eff}}{k_f}\right)Br\,\mathrm{Re}^2\left(\frac{\partial p}{\partial x}\right)^2 s^4 \tag{26}$$

where $\theta$ is the upper wall temperature and the functions of $\omega(y)$ and $M(y)$ are defined as:

$$\omega(y) = -Br\left\{\begin{array}{l}\frac{B_1^2+B_2^2}{4}\cosh\left(\frac{2y}{\sqrt{Da}}\right)-2B_2\,\mathrm{Re}\,Da\frac{\partial p}{\partial x}\cosh\left(\frac{y}{\sqrt{Da}}\right)+ \\ \frac{1}{2}\mathrm{Re}^2\,Da\left(\frac{\partial p}{\partial x}\right)^2 y^2-\frac{B_1\cdot B_2}{2}\left[\sinh\left(\frac{2y}{\sqrt{Da}}\right)-\frac{2y}{\sqrt{Da}}\right]+ \\ 2B_1\,\mathrm{Re}\,Da\frac{\partial p}{\partial x}\sinh\left(\frac{y}{\sqrt{Da}}\right)\end{array}\right\} \tag{27}$$

$$M(y) = -Br\left\{\begin{array}{l}\frac{B_1^2+B_2^2}{2\sqrt{Da}}\sinh\left(\frac{2y}{\sqrt{Da}}\right)-2B_2\,\mathrm{Re}\sqrt{Da}\frac{\partial p}{\partial x}\sinh\left(\frac{y}{\sqrt{Da}}\right)+ \\ \mathrm{Re}^2\,Da\left(\frac{\partial p}{\partial x}\right)^2 y-\frac{2B_1\cdot B_2}{\sqrt{Da}}\sinh^2\left(\frac{y}{\sqrt{Da}}\right)+ \\ 2B_1\,\mathrm{Re}\sqrt{Da}\frac{\partial p}{\partial x}\cosh\left(\frac{y}{\sqrt{Da}}\right)\end{array}\right\} \tag{28}$$

Reynolds number, according to channel width $H$ and maximum velocity, $u_{Max}$ is equal to 180. For numerical simulations, a constant body force is applied to drive fluid in the channel, and the relaxation time $\tau$ is set to 0.75. The porous media thickness is $h=s=H/4$ , and the characteristic length scale in Darcy number is $H/2$. The group parameter ($\Omega$) is set to five in calculations. Non-dimensional temperature graphs for Br=0.02, 0.2, 0.8, 2, Da=0.1 and $\frac{k_{eff}}{k_f} = 5$ are depicted in Fig. 2. As shown in this figure, the effects of viscous dissipation for Br <0.02 are negligible, because temperature in porous media and plain region changes approximately linearly. Fig. 3 shows the entropy generation profiles for different Br numbers. It is evident from this figure that the discontinuity in temperature profiles at the porous-plain interface creates a similar discontinuity in entropy generation number.

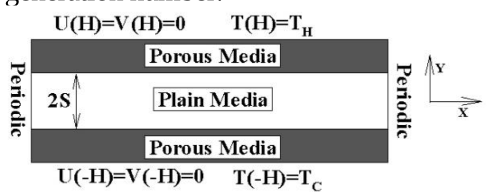


**Fig. 1.** Schematic and boundary conditions of the channel with porous coating on walls

**Channel with porous insert at the canter:** The schematic of the problem and boundary conditions are shown in Fig.4. An analytical solution considering viscous dissipation for these geometries and boundary conditions is obtained. Similar to the previous problem, Eqs. (1-4) are solved here to determine flow and temperature fields. By integrating Eqs. (1-2), velocity profiles in porous and plain regions are obtained. Again, no-slip boundary conditions on the channel walls and continuity of velocity and shear stress on the porous-plane interface are used to calculate six integration constants. The resulting velocity profiles are as follows:

$$u_f = \frac{\mathrm{Re}}{2}\frac{\partial p}{\partial x} y^2 + B_1|y| + B_2 \qquad -1 < y < -\frac{s}{H} \,\&\, \frac{s}{H} < y < 1 \tag{29}$$

$$u_p = C\cosh\left(\frac{y}{\sqrt{Da}}\right) - Da\,\mathrm{Re}\frac{\partial p}{\partial x} \qquad -\frac{s}{H} < y < \frac{s}{H} \tag{30}$$

Where the constants of $C$, $B_1$ and $B_2$ are determined as follows:

$$C = \mathrm{Re}\frac{\partial p}{\partial x}\frac{Da - \frac{s^2}{2} + s - \frac{1}{2}}{\cosh\left(\frac{s}{\sqrt{Da}}\right) + \frac{1-s}{\sqrt{Da}}\sinh\left(\frac{s}{\sqrt{Da}}\right)} \tag{31}$$

$$B_1 = \frac{C}{\sqrt{Da}}\sinh\left(\frac{s}{\sqrt{Da}}\right) - \mathrm{Re}\frac{\partial p}{\partial x}s \tag{32}$$

$$B_2 = -\frac{C}{\sqrt{Da}}\sinh\left(\frac{s}{\sqrt{Da}}\right) + (s-0.5)\,\mathrm{Re}\frac{\partial p}{\partial x} \tag{33}$$

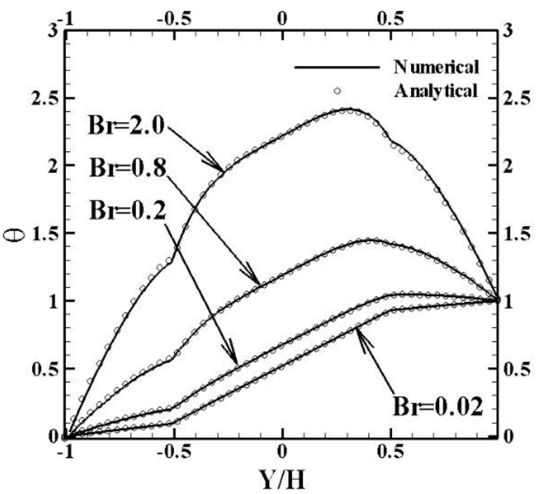


**Fig. 2.** Temperature profiles for channel with porous coating on walls (different Br Numbers).

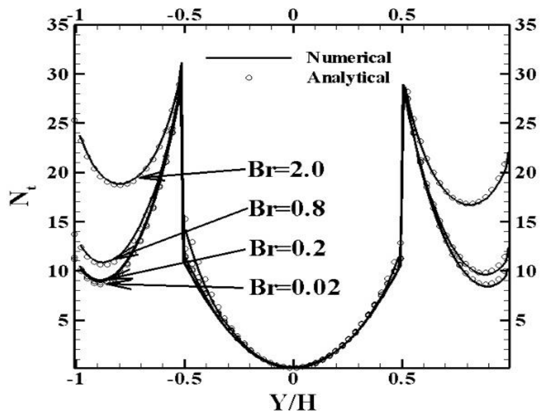


**Fig. 3.** Entropy generation profiles in the channel with porous coating on walls in different Br numbers

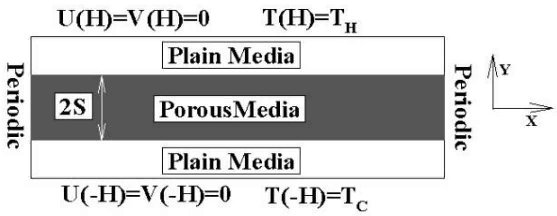


**Fig. 4.** Schematic and boundary conditions of the channel porous insert at the center

Now, the terms of $\partial u/\partial y$ and $u^2$ can be calculated from Eqs. (29-33). By substituting these terms in Eqs. (3-4) and perform integration, the analytical solutions for temperature are obtained as follows:

$$\theta_{fL} = \omega_f(y) + F_1 y + F_2 \qquad -1 < y < -\frac{s}{H} \tag{34}$$

$$\theta_{fH} = \omega_f(y) + E_1 y + E_2 \qquad \frac{s}{H} < y < 1 \tag{35}$$

$$\theta_p = \omega_p(y) + H_1 y + H_2 \qquad -\frac{s}{H} < y < \frac{s}{H} \tag{36}$$

Where $\omega_f(y)$ and $\omega_p(y)$ are calculated as follows:

$$\omega_f(y) = -Br\frac{k_{eff}}{k_f}\left\{\begin{array}{l}\frac{\mathrm{Re}^2}{12}\left(\frac{\partial p}{\partial x}\right)^2 y^4 + \\ \frac{B_1}{3}\mathrm{Re}\frac{\partial p}{\partial x}|y^3| + \frac{B_1^2}{2}y^2\end{array}\right\} \tag{37}$$

$$\omega_p(y) = -Br\left\{\begin{array}{l}\frac{C^2}{4}\cosh\left(\frac{2y}{\sqrt{Da}}\right) - 2C\,\mathrm{Re}\,Da\frac{\partial p}{\partial x}\cosh\left(\frac{y}{\sqrt{Da}}\right) \\ +\frac{1}{2}\mathrm{Re}^2 Da\left(\frac{\partial p}{\partial x}\right)^2 y^2\end{array}\right\} \tag{38}$$

The temperature derivations are computed as follows:

$$\left(\frac{d\theta}{dy}\right)_{fL} = d\omega_f(y) + F_1 \qquad -1 < y < -\frac{s}{H} \tag{39}$$

$$\left(\frac{d\theta}{dy}\right)_{fH} = d\omega_f(y) + E_1 \qquad \frac{s}{H} < y < 1 \tag{40}$$

$$\left(\frac{d\theta}{dy}\right)_p = d\omega_p(y) + H_1 \qquad -\frac{s}{H} < y < \frac{s}{H} \tag{41}$$

Where $d\omega_f(y)$ and $d\omega_p(y)$ are determined as:

$$d\omega_f(y) = -Br\frac{k_{eff}}{k_f}\left\{\begin{array}{l}\frac{\mathrm{Re}^2}{3}\left(\frac{\partial p}{\partial x}\right)^2 y^3 + \\ \frac{B_1}{|y|}\mathrm{Re}\frac{\partial p}{\partial x}y^3 + B_1^2 y\end{array}\right\} \tag{42}$$

$$d\omega_p(y) = -Br\left\{\begin{array}{l}\frac{C^2}{2\sqrt{Da}}\sinh\left(\frac{2y}{\sqrt{Da}}\right) - \\ 2C\,\mathrm{Re}\sqrt{Da}\frac{\partial p}{\partial x}\sinh\left(\frac{y}{\sqrt{Da}}\right) + \\ \mathrm{Re}^2\,Da\left(\frac{\partial p}{\partial x}\right)^2 y\end{array}\right\} \tag{43}$$

The integration constants are calculated by applying temperature and heat flux continuity at the porous-plain interface and constant wall temperature boundary conditions on the channel walls.

$$H_1 = \frac{\theta(1)}{2\left(\frac{k_{eff}}{k_f}\right) + 2\left(1 - \frac{k_{eff}}{k_f}\right)s} \qquad -1 < y < -\frac{s}{H} \tag{44}$$

$$E_1 = \frac{k_{eff}}{k_f}\left(H_1 + d\omega_p(s)\right) - d\omega_f(s) \qquad \frac{s}{H} < y < 1 \tag{45}$$

$$F_1 = \frac{k_{eff}}{k_f}\left(H_1 - d\omega_p(s)\right) + d\omega_f(s) \qquad -\frac{s}{H} < y < \frac{s}{H} \tag{46}$$

$$F_2 = F_1 - \omega_f(1) \tag{47}$$

$$E_2 = \theta(1) - \omega_f(1) - E_1 \tag{48}$$

$$H_2 = \omega_f(s) - \omega_p(s) + (E_1 - H_1)s + E_2 \tag{49}$$

In the above equations, subscripts $f$, $p$, $fH$ and $fL$ represent the fluid region, porous region, upper fluid region, and lower fluid region, respectively. The characteristic length for calculating the Darcy number is $H/2$, and the reference velocity ($U_c$) is 0.1. The applied body force in the present problem ($dp/dx$) is equal to the previous problem (channel with porous coating on its walls) at Da=0.1. Since, body force is kept constant, the Reynolds number (based on channel width and maximum velocity) is changed with the Darcy number. For instance, the resulting Reynolds numbers for Darcy numbers 0.001, 0.01, and 0.1 are 45, 46, and 60, respectively. Similar to the calculations for channels with porous coating on the walls, the relaxation time $\tau$ is set to 0.75, and the porous media layer thickness ($s$) is equal to $H/2$. Figure 5 shows the non-dimensional temperature profiles in Da=0.1 and $k_{eff}/k_f = 5$. The curves are plotted in four different Br numbers Br=0.02, 0.2, 0.8, and 2. It can be seen in this figure that the analytical and numerical results are identical. Figure 6 shows the entropy generation number $N_t$. As shown in this figure, there is a very good agreement between numerical and analytical results.

**Fully Filled Channel:** The schematic and boundary conditions for the present problem are depicted in Fig.7. By solving the momentum equation in porous media (Eq. 1) and implementing the no-slip boundary condition on the channel wall, we have:

$$u = -Da\,Re\left(\frac{\partial p}{\partial x}\right)\left[1 - \frac{Cosh\left(y/\sqrt{Da}\right)}{Cosh\left(1/\sqrt{Da}\right)}\right] \tag{50}$$

By substituting velocity ($u$) and its derivative ($\partial u/\partial y$) in the non-dimensional energy equation (Eq. 3), we have:

$$\theta = -Br\,Da\,\mathrm{Re}^2\left(\frac{\partial p}{\partial x}\right)^2\left\{\begin{array}{l}\frac{1}{2}y^2 - \frac{2Da\,\mathrm{Cosh}\left(y/\sqrt{Da}\right)}{\mathrm{Cosh}\left(1/\sqrt{Da}\right)} + \\ \frac{Da\,\mathrm{Cosh}^2\left(y/\sqrt{Da}\right)}{2\,\mathrm{Cosh}^2\left(1/\sqrt{Da}\right)}\end{array}\right\} + \frac{y}{2} + \frac{1}{2}\left(1 + Br\,Da\,\mathrm{Re}^2\left(\frac{\partial p}{\partial x}\right)^2[1 - 3Da]\right) \tag{51}$$

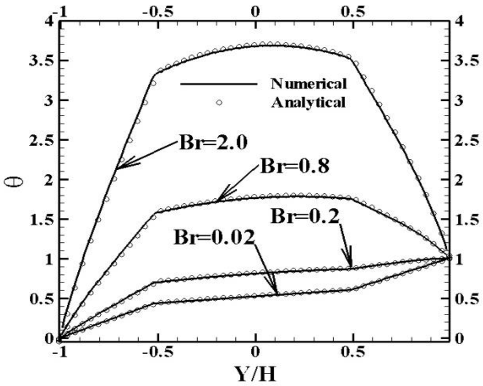


**Fig. 5.** Non-dimensional temperature profiles in the channel with porous insert at center for different Br Numbers.

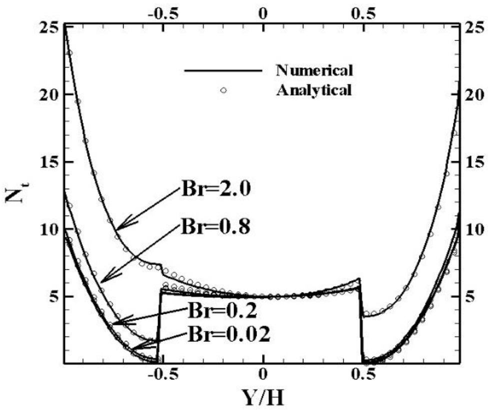


**Fig. 6.** Entropy generation profiles in the channel with porous insert at center for different Br numbers

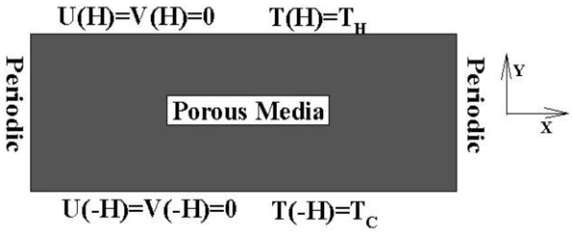


**Fig. 7.** Schematic and boundary conditions of channel fully filled with porous media.

After calculating temperature and velocity profiles, the entropy generation number is calculated as follows:

$$N_s = \left(\frac{\partial \theta}{\partial y}\right)^2 + \frac{Br}{\Omega}\left[\frac{u^2}{Da} + \left(\frac{\partial u}{\partial y}\right)^2\right] \quad (52)$$

Where the derivatives $\frac{\partial \theta}{\partial y}$ and $\frac{\partial u}{\partial y}$ are as follows:

$$\left(\frac{\partial u}{\partial y}\right) = -\sqrt{Da}\,\mathrm{Re}\left(\frac{\partial p}{\partial x}\right)\left[\frac{Sinh\left(y/\sqrt{Da}\right)}{Cosh\left(1/\sqrt{Da}\right)}\right] \quad (53)$$

$$\left(\frac{\partial \theta}{\partial y}\right) = \frac{1}{2} - BrDa\,\mathrm{Re}^2\left(\frac{\partial p}{\partial x}\right)^2 \times \left\{ y - \frac{2\sqrt{Da}\,\mathrm{Sinh}\left(y/\sqrt{Da}\right)}{\mathrm{Cosh}\left(1/\sqrt{Da}\right)} + \frac{\sqrt{Da}\,\mathrm{Cosh}\left(y/\sqrt{Da}\right)\mathrm{Sinh}\left(y/\sqrt{Da}\right)}{\mathrm{Cosh}^2\left(1/\sqrt{Da}\right)} \right\} \quad (54)$$

The Reynolds number, according to channel width ($H$) and maximum velocity ($U_c$), is 180. The characteristic length scale in the Darcy number is the channel width ($H$). In numerical simulations, the applied body force is such that the maximum velocity for relaxation time $\tau = 0.75$ is 0.1. Figure 8 shows the non-dimensional temperature profiles in Da=0.1, Br=0.02, 0.2, 0.8, 2, and $k_{eff}/k_f = 5$. Based on this Figure, we can verify the performance of both numerical and analytical methods to simulate the effects of viscous dissipation.

Figure 9 shows the entropy generation number $N_t$ in the mentioned Br numbers for Da=0.1 and $\Omega = 0.2$. This Figure illustrates very good agreement between numerical and analytical results.

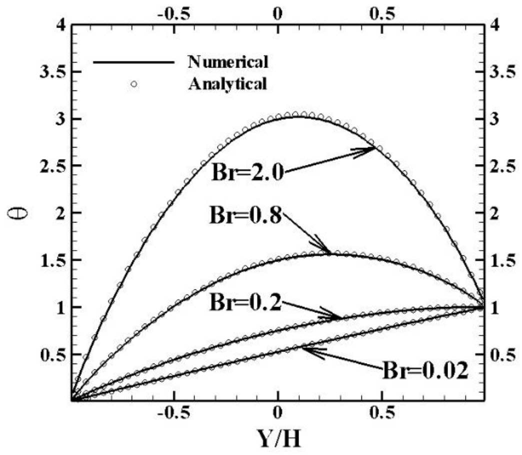


**Fig. 8.** Temperature profiles in a channel fully filled with porous media in different Br Number.

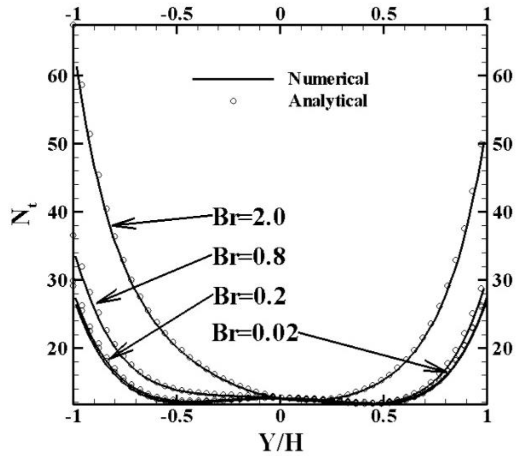


**Fig. 9.** Entropy generation profiles in a channel fully filled with porous media in different Br numbers

## 4 RESULTS AND DISCUSSION

In this section of the article, the results of the analytical solutions for three-channel geometries (porous media coating on the channel walls, porous layer inserted in the channel center, and porous media occupying the whole of the channel) are analyzed and compared with each other. These results include the impact of Br, Da, and the porous media thickness on the Be and entropy generation Number. The non-dimensional pressure gradient is kept constant in all calculations. This constant pressure gradient corresponds to Re=180 for the channel with porous coating on its walls (where Da=0.1 and S=0.25). Note that the Reynolds number is based on the maximum velocity and the channel width.

**Channel with Porous Coating on Walls:** In this section, the effects of Darcy number, Brinkman number, and the porous layer thickness on Bejan and entropy generation numbers for the channel with porous media coating on its walls are explained.

Figures 10 and 11 represent the non-dimensional velocity and temperature profiles across channel width for different Da numbers at Br=5. As shown in Fig. 10, as the Da number increases, since the pressure gradient is constant, the fluid velocity in porous media increases, too. The higher fluid velocity in porous media results in a higher average temperature (Fig. 11) due to the viscous dissipation term in the energy equation.

As is observed in Fig.10, by increasing the porous media thickness from 0.25 to 0.75, the fluid velocity inside and outside of the porous layer is reduced. This velocity reduction causes lower energy conversion due to viscous dissipation, leading to lower average temperature (Fig. 11) and heat transfer rate to the walls.

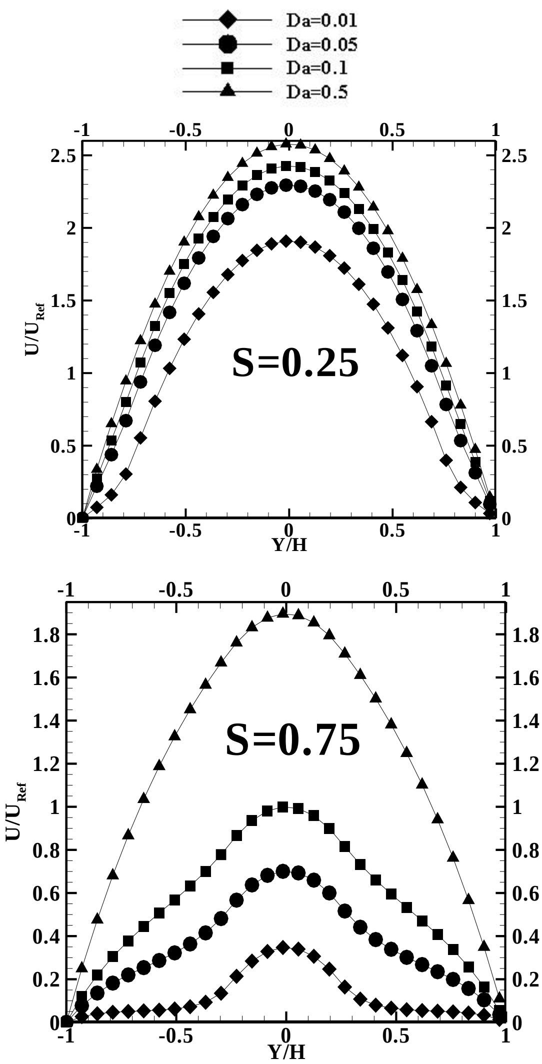


**Fig. 10.** Velocity profiles in the channel with porous media coating on walls in different Da numbers.

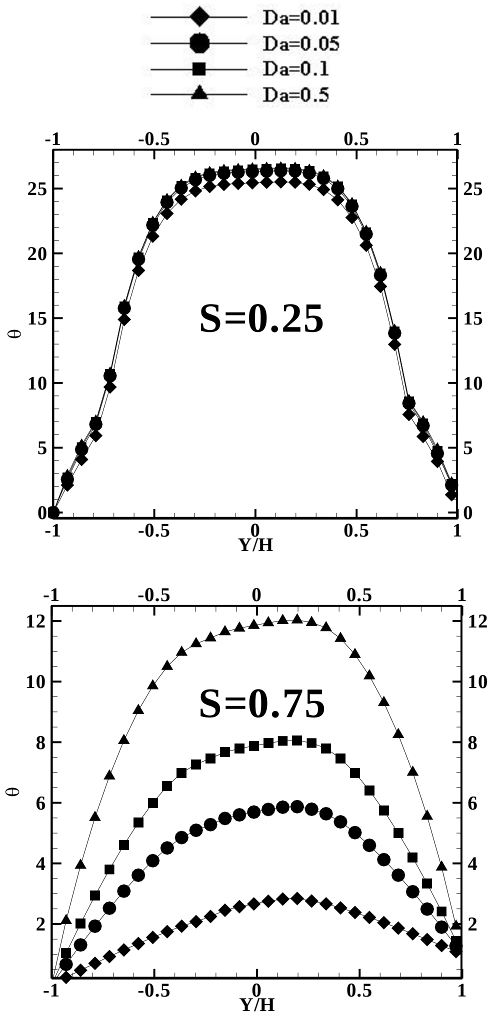


**Fig.11.** The temperature profiles in the channel with porous media coating on walls for Br = 5 and different Da numbers.

The averaged entropy generation number graphs versus Brinkman number in various Da numbers for three porous media thicknesses are depicted in Fig. 12. As shown in this figure, by increasing the Br number, the entropy generation number increases, too. Because by increasing the Br number, more kinetic energy is converted into heat, and the average temperature gradient increases. The higher heat transfer rate and viscous dissipation lead to more irreversibility and entropy generation.

As it was discussed in the previous section, increasing the Da number leads to higher fluid velocity and viscous dissipation, which increases the entropy generation number. Thus, as shown in Fig. 12, the entropy generation number rises by increasing Da number.

Based on Fig. 12, for the porous layer thickness of S=0.5 and S=0.75, the slope of the entropy generation number graphs is steeper for higher Da numbers. This behavior becomes more pronounced at higher Br numbers and thicker porous layers. This can be due to the strengthening of the viscous dissipation in large Br numbers, which increases the graph's sensitivity to the Da number variations.

To show the effects of Da and Br numbers on Bejan number, the Bejan number graphs in three different porous media thicknesses and four different Da numbers are depicted in Fig. 13.

As indicated in Figure 13, by increasing the Br number, the Bejan number increases for all porous media thicknesses and Da numbers examined here. Therefore, it can be concluded that, by increasing the Br number, the contribution of heat transfer in entropy generation increases (compared to the viscous losses). Whereas the contribution of viscosity in entropy generation is dominant for small Br numbers (e.g., Br <1.5 for the S = 0.5).

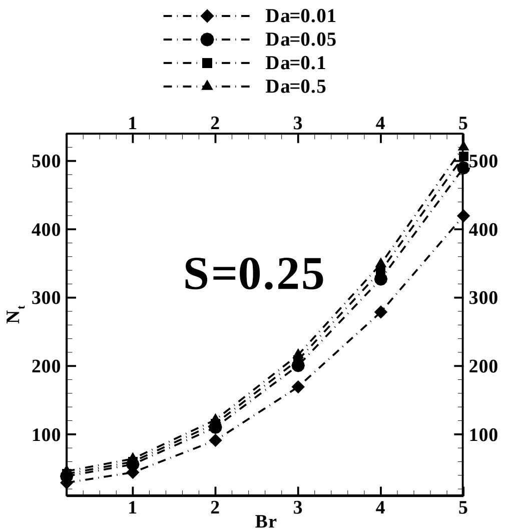


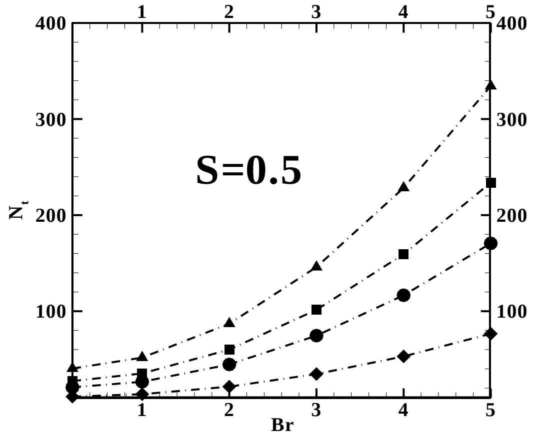


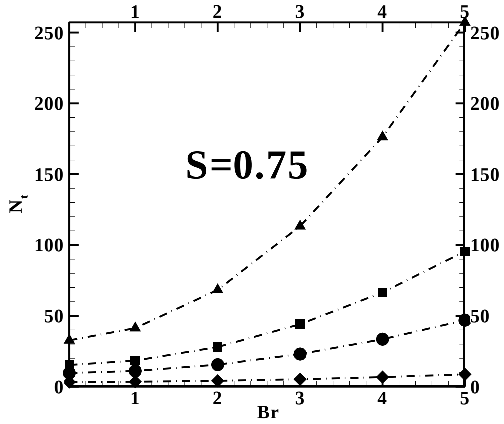


**Fig. 12.** Entropy generation number against Br number in channel with porous media coating on the walls in different Da numbers

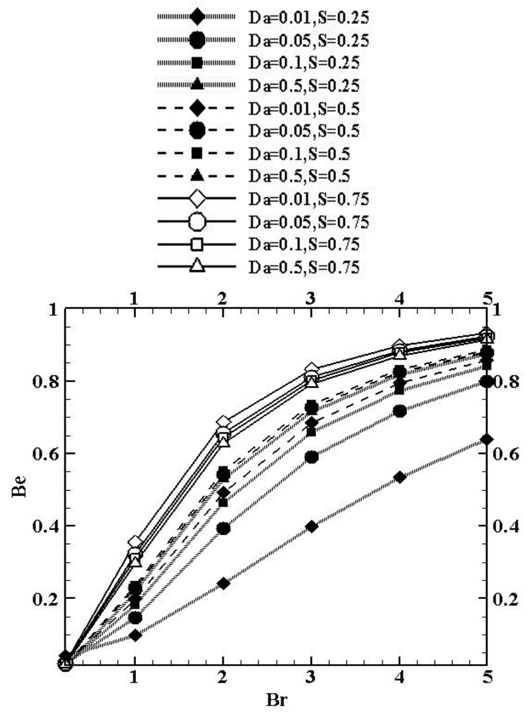


**Fig. 13.** Bejan number graphs versus Br number in channel with porous media coating on walls in different porous media thicknesses and different Da numbers

The effects of the Da number on the Bejan number are completely dependent on the porous media thickness. For instance, in S=0.75, the Bejan number increases by increasing Da number, whereas in S=0.25, the reverse is true, and in S=0.5, the Bejan number graphs are very close to each other. Thus, the transition occurs in the porous media thicknesses near S=0.5. Moreover, the sensitivity of the Bejan number to the Da number reduces with increasing porous media thickness.

**Channel with a Porous Insert Placed at the Canter**:

In this section, the influences of Da number, Br number, and the porous media thickness on Bejan and entropy generation numbers for the channel with a porous insert placed at the canter are explained.

Figures 14 and 15 show the variation of velocity and temperature profiles concerning the Da number for the channel with a porous insert at the core for Br = 5 and two porous insert thicknesses of 0.25 and 0.75. As indicated in these figures, since the pressure gradient is fixed in all cases, the mean velocity and temperature increase with the Da number due to lower flow resistance inside the porous layer.

In comparison with the side porous channel, the velocity and temperature profiles for the core porous channel are more sensitive to Da number variations. As Shown in Figs. 14-15, even for low porous layer thicknesses (S=0.25), the effects of Da number are significant.

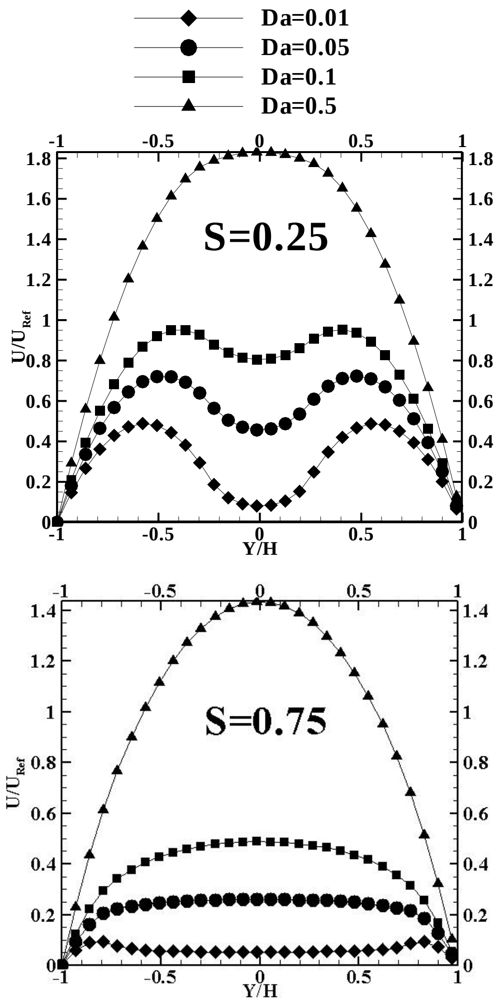


**Fig.14.** Velocity profiles in the channel with porous insert at center in different Da numbers.

The graphs of averaged entropy generation number versus Br number in various Da numbers for three porous media thicknesses are illustrated in Fig. 16. Similar to the entropy generation number versus Br number graphs for side porous channel (Fig. 12), for all studied porous layer thicknesses and Da numbers, the entropy generation number for core porous channel increased as Br and Da numbers raised. This looks reasonable based on velocity and temperature profiles in Figs. 14 and 15, where velocity, velocity gradient, temperature, and temperature gradients (factors affecting the entropy generation) are increased with Da number. Moreover, as indicated in this figure (Fig. 16), the maximum entropy generation number occurs in S=0.25.

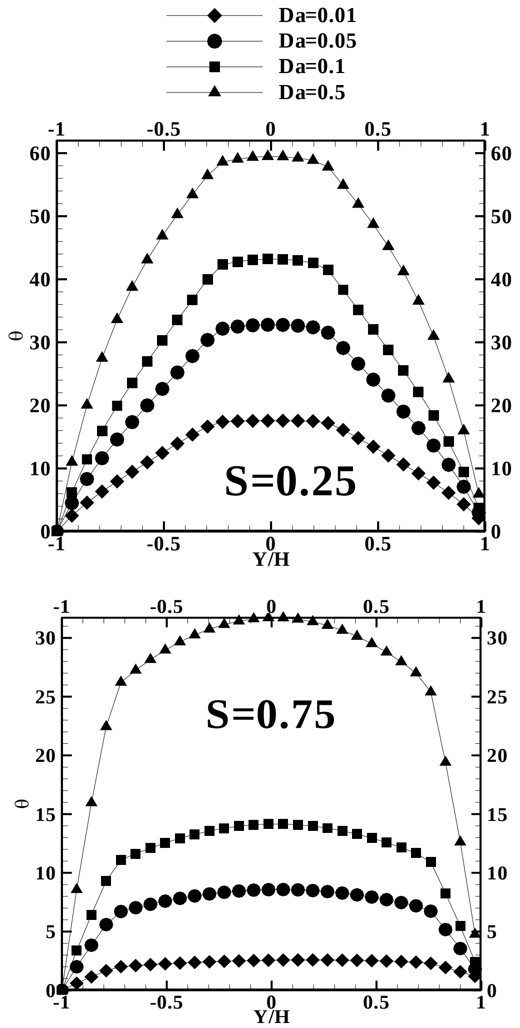


**Fig. 15.** The temperature profiles in the channel with porous insert at the center for Br = 5 and different Da numbers.

The effects of Da number, Br number, and porous media thickness on the Bejan number for three porous media thicknesses are presented in

Fig. 17. As shown in this figure, by increasing the Br number, the Bejan number is raised in all porous media thicknesses examined here. This indicates that the contribution of heat transfer to the entropy generation increases with the Br number. According to Fig. 17, for the Br numbers smaller than 1, the Bejan numbers for approximately all Da numbers and porous layer thicknesses examined here are less than 0.5. This indicates that the contribution of viscosity and drag forces in entropy generation is dominant for Br<1, and for Br numbers less than 0.25, the effects of heat transfer in entropy generation can be neglected approximately. Additionally, in all porous media thicknesses, the Bejan number increases with the Da number. Thus, the contribution of heat transfer to the entropy generation increases with the Da number. By reduction in porous media thickness, the sensitivity of the Bejan number to changes in the Da number reduces. As can be seen in S=0.25, the Da number changes do not have a significant impact on the Bejan number.

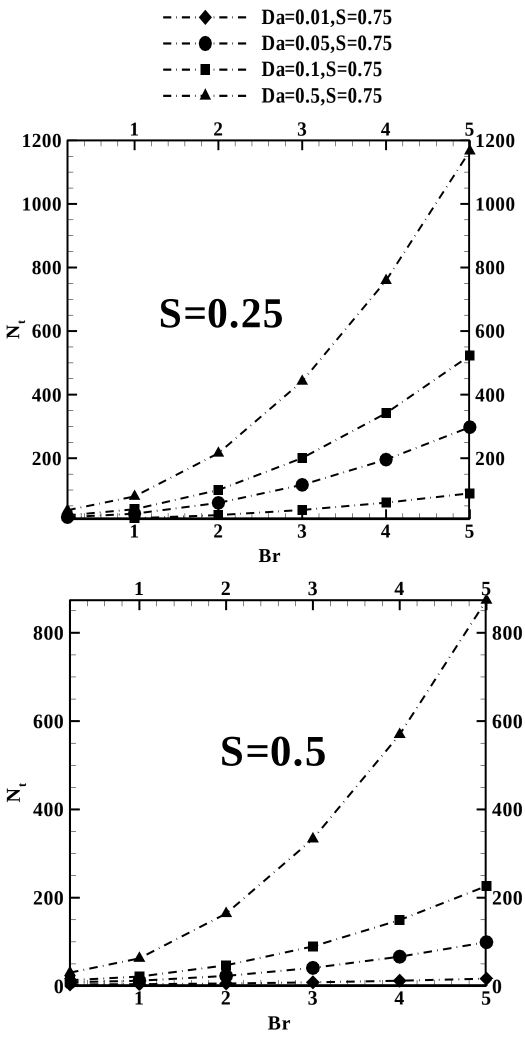


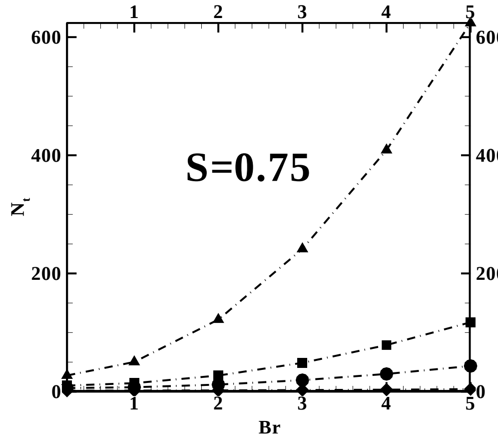


**Fig. 16.** The entropy generation number versus Br number in the channel with porous insert at the center for different Da numbers.

As shown in Fig. 17, the Bejan number reduces with increasing porous media thickness, which is more obvious in low Da numbers. This reflects the fact that when the porous media thickness increases, the contribution of heat transfer in entropy generation reduces (especially in low Da numbers).

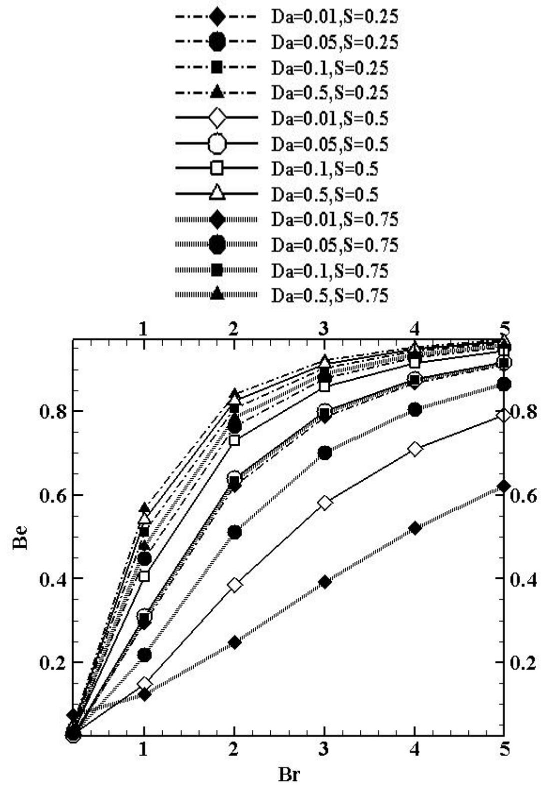


**Fig. 17.** Bejan number graphs versus Br number in channel with porous insert at center in different porous media thicknesses and different Da numbers

**Results of Channel Fully Filled with Porous Media:** In this section of the article, the influences of Da and Br numbers on Bejan and entropy generation numbers in a channel fully filled with porous media are investigated.

Figures 18 and 19 present velocity and temperature profiles across the channel for Br = 5 and different Da numbers. As shown in these figures, the averaged velocity, averaged temperature, near-wall velocity, and temperature gradients increase with increasing Da number.

The graphs of averaged entropy generation number versus Br number for different Da numbers for the channel fully filled with porous media are shown in Fig. 20. As shown in this figure, the entropy generation number increases as Br and Da numbers increase (same as side and mid porous channels in Figs. 16 and 12). Based on Fig. 18, by increasing the Da number, the averaged velocity and its gradient in porous media increase, which causes an increase in the irreversibility due to viscosity. Similarly, according to Fig. 19, an increase in velocity and its gradient increases the average temperature and heat transfer rate, so irreversibility due to heat transfer increases. Moreover, as shown in Fig. 20, the growth rate of the entropy generation number increases with increasing Br and Da numbers.

Bejan number graphs against the Br number for the full porous channel in different Da numbers are shown in Fig. 21. As expected, by increasing the Br number, the contribution of heat transfer in entropy generation increases as the Bejan number rises. As shown in this figure, for all studied Da numbers, the Bejan number is smaller than 0.5, and for Br numbers, it is less than 3. Additionally, for Br numbers less than 0.5, the irreversibility due to heat transfer can be ignored approximately. Comparing this result with that presented in Figs. 13 and 17 for side porous and mid-porous channels indicates that the Bejan number of full porous channels is less than that of partially filled channels. Thus, the impact of hydrodynamic irreversibility for the full porous channel is more significant among the three-channel geometries studied here.

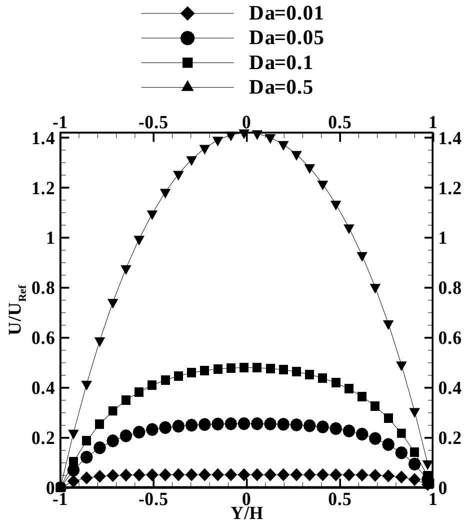


**Fig. 18.** Velocity profiles in a channel fully filled with porous media in different Da numbers.

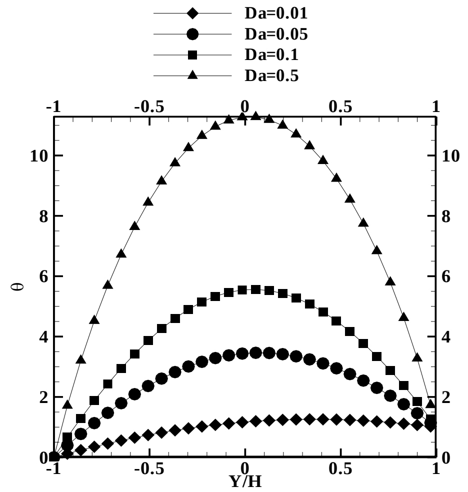


**Fig. 19.** Temperature profiles in channel fully filled with porous media for Br=5 in different Da numbers.

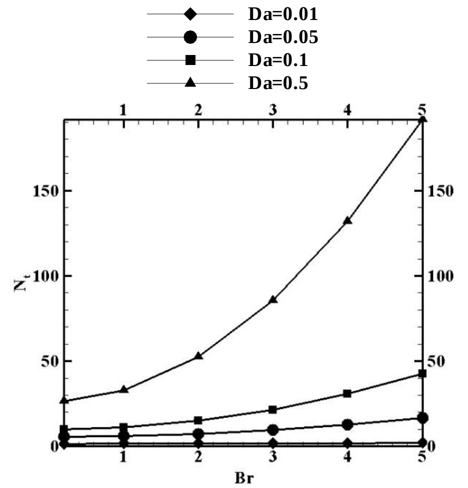


**Fig. 20.** The entropy generation number versus the Br number in the channel fully filled with porous media for different Da numbers.

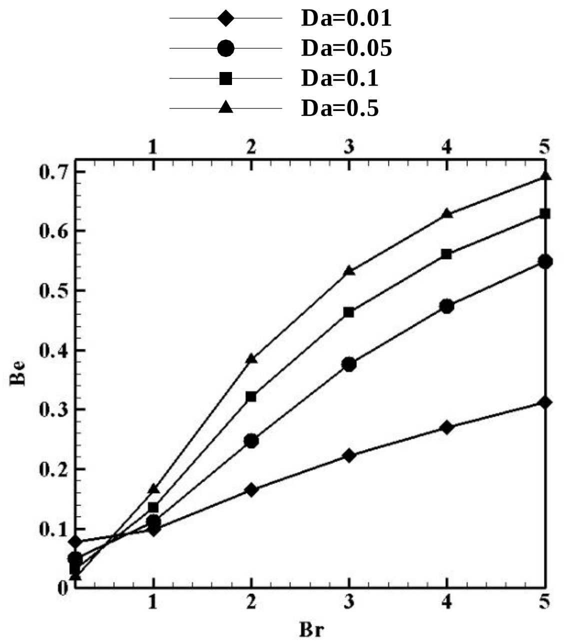


**Fig. 21.** Bejan number graphs versus Br number in channel fully filled with porous media for different Da numbers.

## 5 CONCLUSION

In this research, we proposed some analytical solutions for velocity, temperature, entropy generation number, and Bejan number profiles in a thermally fully developed porous channel. The effects of viscous dissipation were included, and three channel geometries of side porous, mid porous, and full porous were studied. Our analytical results were compared with the numerical results of the well-known Lattice Boltzmann Method (LBM), which showed very close agreement. By comparison, the results of this research can be concluded as follows:

- The entropy generation number of the side porous channel is considerably lower than the entropy generation number of the mid-porous channel under the same conditions (same Da number, Br number, and porous media thickness).
- The Bejan number of full porous channels, even at high Br numbers, is the lowest among the three geometries studied here. This shows that the share of viscosity in entropy generation (particularly for Br numbers smaller than 3) is more than that of heat transfer.
- The sensitivity of the entropy generation and Bejan numbers graphs to the Br number in all three geometries is noticeable. Thus, it is very important to consider the Br number in this kind of problem.

## CONFLICT OF INTEREST

No potential conflict of interest was reported by the authors.

## REFERENCES

[1] P.X. Jiang, M. Li., T.J. Lu., L. Yu., and Ren, Z.P. “Experimental Research on Convection Heat Transfer in Sintered Porous Plate Channels”. *International Journal of Heat and Mass Transfer*, vol. 47, pp.2085–2096, 2004, https://doi.org/10.1016/j.ijheatmasstransfer.2003.12.004.

[2] P.X. Jiang, and X.C. Lu. “Numerical Simulation of Fluid Flow and Convection Heat Transfer in Sintered Porous Plate Channels”. *International Journal of Heat and Mass Transfer*, vol. 4, pp. 1685–1695, 2006, https://doi.org/10.1016/j.ijheatmasstransfer.2005.10.026.

[3] A. Bejan, “A Study of Entropy Generation in Fundamental Convective Heat Transfer”, *J. Heat Transfer*, vol. 101, pp. 718–725, 1979, https://doi.org/10.1115/1.3451063.

[4] A. Bejan, “Fundamentals of Exergy Analysis, Entropy Generation Minimization, and the Generation of Flow Architecture”, *Int. J. Energy Res*, vol. 26, pp. 545-565, 2002, https://doi.org/10.1002/er.804.

[5] S.H. Tasnim, S. Mahmud, M.A.H., Mamun, “Entropy Generation in a Porous Channel with Hydromagnetic Effect”, *Exergy, an International Journal*, vol. 2, pp. 300–308, 2002, https://doi.org/10.1016/S1164-0235(02)00065-1.

[6] N. Allouache and S. Chikh, “Thermodynamic Analysis in a Parallel Flow Annular Heat Exchanger”, *European Congress on Computational Methods in Applied Sciences and Engineering, ECCOMAS*, 2004, 10.1016/j.icheatmasstransfer.2020.105005.

[7] T.V. Morosuk, “Entropy Generation in Conduits Filled with Porous Medium Totally and Partially”, *International Journal of Heat and Mass Transfer*, vol. 48, pp. 2548–2560, 2005, https://doi.org/10.1016/j.ijheatmasstransfer.2005.01.018.

[8] A. Mohamed, W.M. Teamah, M. El-Maghlany, and D. Khairat, “Numerical Simulation of Laminar Forced

Convection in Horizontal Pipe Partially or Completely Filled with Porous Material", *International Journal of Thermal Sciences*, vol. 50, pp. 1512-1522, 2011, 10.1016/j.ijthermalsci.2011.03.003.

[9] D.S. Cimpean and I. Pop, "A Study of Entropy Generation Minimization in an Inclined Channel", Wseas Transactions On Heat And Mass Transfer, vol. 6, Issue 2, April 2011, ISSN: 1790-5044.

[10] K. Hooman, "A Perturbation Solution for Forced Convection in a Porous-Saturated Duct", *Journal of Computational and Applied Mathematics*, vol. 211, pp. 57 – 66, 2008, https://doi.org/10.1016/j.cam.2006.11.005.

[11] D. A. Nield, "Resolution of a paradox Involving Viscous Dissipation and Nonlinear Drag in a Porous Medium", *Transport in Porous Media*, vol. 41, pp. 349–357, 2000, https://doi.org/10.1023/A:1006636605498.

[12] S. Mahmud, and R.A. Fraser, "Flow, Thermal, and Entropy Generation Characteristics inside a Porous Channel with Viscous Dissipation", *International Journal of Thermal Sciences*, vol. 44, pp. 21–32, 2005, 10.1016/j.ijthermalsci.2004.05.001

[13] K. Hooman, and A. Ejlali, "Entropy Generation for Forced Convection in a Porous Saturated Circular Tube with Uniform Wall Temperature", *International Communications in Heat and Mass Transfer*, vol. 34, pp. 408–419, 2007, 10.1016/j.icheatmasstransfer.2006.10.008

[14] K., Hooman and A.A. Ranjbar-Kani, "A Perturbation Based Analysis to Investigate Forced Convection in a Porous Saturated Tube", *Journal of Computational and Applied Mathematics*, vol. 162, pp. 411–419, 2004, https://doi.org/10.1016/j.cam.2003.08.031

[15] H. Abbassi, "Entropy Generation Analysis in a Uniformly Heated Microchannel Heat Sink", *energy*, vol. 32, pp.1932–1947, 2007, https://doi.org/10.1016/j.energy.2007.02.007.

[16] K. Hooman, A. Ejlali, and F. Hooman, "Entropy Generation Analysis of Thermally Developing Forced Convection in Fluid-Saturated Porous Medium", *Appl. Math. Mech.-Eng*, vol. 29, pp. 229–237, 2008, https://link.springer.com/article/10.1007/s10483-008-0210-1

[17] D. S. Chauhan and V. Kumar, "Effects of Slip Conditions on Forced Convection and Entropy Generation in a Circular Channel Occupied by a Highly Porous Medium: Darcy Extended Brinkman-Forchheimer Model", *Turkish J. Eng. Env. Sci.*, vol. 33, pp. 91 – 104, 2009.

[18] D.S. Chauhan and V. Kumar, "Heat Transfer and Entropy Generation During Compressible Fluid Flow in a Channel Partially Filled with a Porous Medium", *International Journal of Energy & Technology*, vol. 3, pp. 1-10, 2011.

[19] D.S. Chauhan and V. Kumar, "Entropy Analysis for Third-Grade Fluid Flow with Temperature-Dependent Viscosity in Annulus Partially Filled with Porous Medium", *Theoret. Appl. Mech.*, vol. 40, Issue 3, pp. 444-464, 2013, https://doi.org/10.2298/TAM1303441C

[20] O.D. Makinde, and A.S. Eegunjobi, "Effects of Convective Heating on Entropy Generation Rate in a Channel with Permeable Walls", *Entropy*, vol. 15, pp. 220-233, 2013, https://doi.org/10.3390/e15010220.

[21] F. Kamish, "Analysis of Laminar Flow and Forced Convection Heat Transfer in a Porous Medium", *Transp. Porous Med.*, vol. 80, pp. 345–371, 2009, https://doi.org/10.1007/s11242-009-9364-7.

[22] K. Hooman, F. Hooman, and S.R. Mohebpour, "Entropy Generation for Forced Convection in a Porous Channel with Isoflux or Isothermal Walls", *Int. J. Exergy*, vol. 5, pp. 78–96, 2008, https://doi.org/10.1504/IJEX.2008.016014

[23] M. R. Salimi, M. Taeibi-Rahni, and F. Jam. "Heat transfer analysis of a porously covered heated square cylinder, using a hybrid Navier–Stokes–lattice Boltzmann numerical method." *International Journal of Thermal Sciences*, vol. 91, pp. 59-75, 2015, 10.1016/j.ijthermalsci.2015.01.004.

[24] M. R. Salimi, M. Taeibi Rahni, and F. Jam. "Pore-scale simulation of fluid flow passing over a porously covered square cylinder located at the middle of a channel, using a hybrid MRT-LBM–FVM approach." *Theoretical and Computational Fluid Dynamics*, vol. 29, pp. 171-191, 2015, https://doi.org/10.1007/s00162-015-0347-8.

[25] M. R. Salimi, and M. Taeibi-Rahni. "New lifting relations for estimating LBM distribution functions from corresponding macroscopic quantities, based on equilibrium and non-equilibrium moments." *Journal of Computational Physics*, vol. 302, pp. 155-175, 2015, 10.1016/j.jcp.2015.08.045.

[26] M. R. Salimi, E. Alizadeh-Seresht, and M. Taeibi-Rahni. "New hybrid finite volume-thermal lattice Boltzmann method, based on multi relaxation time collision operator." *International Journal of Heat and Mass Transfer*, vol. 138, 1281-1294, 2019, 1281-1294, https://doi.org/10.1016/j.ijheatmasstransfer.2019.04.130.

[27] M. R. Salimi, M. Taeibi-Rahni, and H. Rostamzadeh. "Heat transfer and entropy generation analysis in a three-dimensional impinging jet porous heat sink under local thermal non-equilibrium condition." *International Journal of Thermal Sciences*, vol. 153, Art. No. 106348, 2020, 10.1016/j.ijthermalsci.2020.106348.

[28] H. Rostamzadeh, M. R. Salimi, and M. Taeibi-Rahni. "Permeability correlation with porosity and Knudsen number for rarefied gas flow in Sierpinski carpets." *Journal of Natural Gas Science and Engineering*, vol. 56 pp. 549-567, 2018, 10.1016/j.jngse.2018.06.037.

[29] H. Rostamzadeh, M. R. Salimi, and M. Taeibi-Rahni. "Pore-scale modeling of rarefied gas flow in fractal micro-porous media, using lattice Boltzmann method (LBM)." *Journal of Thermal Analysis and Calorimetry*, vol. 135, 1931-1942, 2019, https://doi.org/10.1007/s10973-018-7401-x.

[30] F. Abdalla Zahor, and et al. "Modeling entropy generation of magnetohydrodynamics flow of nanofluid in a porous medium: a review." *International Journal of Numerical Methods for Heat & Fluid Flow*, vol. 33, no. 2, pp. 751-771, 2023, https://doi.org/10.1108/HFF-05-2022-0266

[31] F. Mebarek-Oudina, and et al. "Hybrid-nanofluid magneto-convective flow and porous *media contribution to entropy generation." International Journal of Numerical Methods for Heat & Fluid Flow*, vol. 34, no. 2, pp. 2024, https://doi.org/10.1108/HFF-06-2023-0326

[32] Bejan, A., "Second Law Analysis in Heat Transfer", *energy*, vol. 5, issues 8-9, pp. 720-732, 1980, https://doi.org/10.1016/0360-5442(80)90091-2.

[33] A.K. Al-Hadhrami, L. Elliott, and D.B. Ingham, "A New Model for Viscous Dissipation in Porous Media Across a Range of Permeability Values", *Transport Porous Media*, vol. 53, 2003, pp. 117–122, https://doi.org/10.1023/A:1023557332542.

[34] D. Nield, and A. Bejan, *Convection in Porous Media*, Third Edition, Springer, New York, 2006.

**COPYRIGHTS**

Authors retain the copyright and full publishing rights.
Published by Iranian Aerospace Society. This article is an open access article licensed under the Creative Commons Attribution 4.0 International (CC BY 4.0).

OPEN ACCESS

**HOW TO CITE THIS ARTICLE**

M. R. Salimi, "Effect of Viscous Heating on Heat Transfer and Entropy Generation inside a Partially Filled Porous Channel," *Journal of Aerospace Science and Technology*, Vol. 18, Issue 2, 2025, pp. 110-126.

DOI: https://doi.org/10.22034/jast.2025.487848.1212

URL: https://jast.ias.ir/article_230228.html